WSRC-RP-89-25

PROBABILISTIC EVALUATION OF MAIN COOLANT PIPE BREAK INDIRECTLY INDUCED BY EARTHQUAKES: SAVANNAH RIVER PROJECT L&P REACTORS (U)

by

S. A. Short and D. A. Wesley
Impell Corporation
Mission Viejo, CA

N. G. Awadalla
Westinghouse Savannah River Company
Savannah River Site
Aiken, SC

and

R. P. Kennedy
RPK Structural Mechanics Consulting
Yorba Linda, CA

A paper proposed for presentation
Second DOE Natural Phenomena Hazards Mitigation Conference
Knoxville, TN
October 3-5,1989

and for publication in the conference proceedings

PROBABILISTIC EVALUATION OF MAIN COOLANT PIPE BREAK INDIRECTLY INDUCED BY EARTHQUAKES SAVANNAH RIVER PROJECT L & P REACTORS (U)

Stephen A. Short and Donald A. Wesley
Impell Corporation
Mission Viejo, California

Nabil G. Awadalla
Westinghouse Savannah River Company
Aiken, South Carolina

Robert P. Kennedy
RPK Structural Mechanics Consulting
Yorba Linda, California

ABSTRACT

A probabilistic evaluation of seismically-induced indirect pipe break for the Savannah River Project (SRP) L- and P-Reactor main coolant (process water) piping has been conducted. Seismically-induced indirect pipe break can result primarily from: 1) failure of the anchorage of one or more of the components to which the pipe is anchored; or 2) failure of the pipe due to collapse of the structure. The potential for both types of seismically-induced indirect failures was identified during a seismic walkdown of the main coolant piping. This work involved: 1) identifying components or structures whose failure could result in pipe failure; 2) developing seismic capacities or "fragilities" of these components; 3) combining component fragilities to develop plant damage state fragilities; and 4) convolving the plant seismic fragilities with a probabilistic seismic hazard estimate for the site in order to obtain estimates of seismic risk in terms of annual probability of seismic-induced indirect pipe break.

INTRODUCTION

A probabilistic evaluation of pipe break for the Savannah River Project (SRP) L- and P-Reactor main coolant (process water) piping has been conducted. This paper covers the portion of this effort including the evaluation of seismically-induced indirect pipe break. L- and P-Reactors are very similar structures with nearly identical equipment which might affect main coolant loop piping. The P-Reactor building is much weaker than the L-Reactor building in the local region which governs building fragility such that overall seismic risk is somewhat higher for P-Reactor. The L-Reactor evaluation is primarily described herein with results for both L- and P-Reactors presented at the end of the paper.

FRAGILITY METHODOLOGY

The seismic risk of indirect reactor main coolant (RCL) pipe break involves consideration of the seismic capacities (fragilities) of the important components and structures. These components were identified based on discussions with the SRP staff, review of L- and P-Reactor drawings, and plant walkdowns conducted by Drs. R. P. Kennedy and D. A. Wesley. The main tank, main coolant (Bingham) pumps, and the heat exchangers are all of sufficient mass that failure was conservatively considered to result in failure of the pipe. The location of these components as well as the general plant configuration is shown in Figure 1.

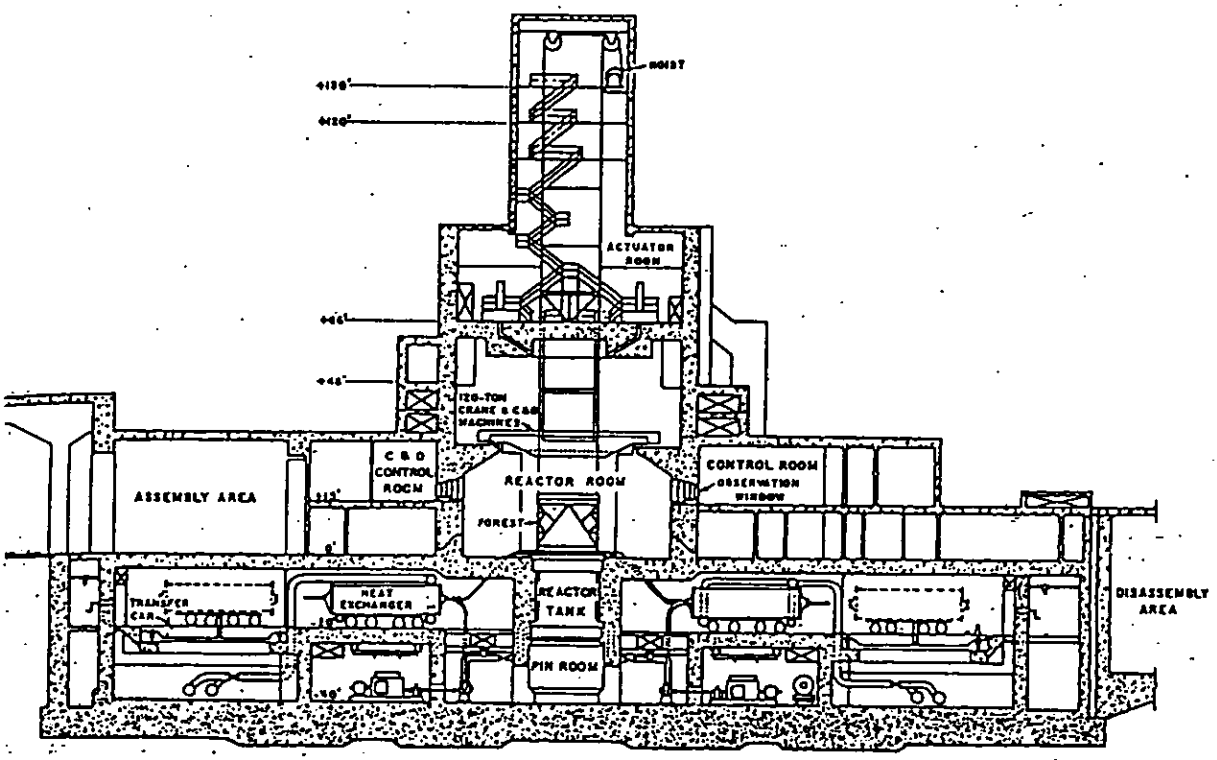

Figure 1 - SRP Reactor Building Configuration

Failure of the building structure above Elevation 0 as well as failure of the forest support and control rod system was investigated due to the potential for impact-induced pipe failure of the exposed nozzles located above the operating floor slab at Elevation 0. Failure of the building structure below Elevation 0 was not considered credible at the seismic levels which govern the indirect pipe break plant risk.

The seismic fragilities and resulting plant risk developed in this investigation are based on breach of the fluid boundary. The approach to developing the conditional probability of RCL pipe break is based on combining the failure probabilities of individual structures and components. Component fragilities are treated as independent which gives a conservative bound on the combined probability of seismic indirect pipe break. Fragility curves must be developed primarily from analysis combined heavily with engineering judgment supported by very limited test data. Such fragility curves will contain a great deal of uncertainty, which must be recognized. Because of this uncertainty, great precision in attempting to define the shape of these curves is unwarranted. Thus, a procedure which requires a minimum amount of information, incorporates uncertainty into the fragility curves, and easily enables the use of engineering judgment was used.

The entire fragility curve for any mode of failure and its uncertainty can be expressed in terms of the median ground acceleration capacity, $\hat{A}$, and logarithmic standard deviations of the inherent randomness (failure fraction) about the median and the uncertainty (probability) in the median value, β_R and β_U, respectively. Inherent randomness is associated primarily with the earthquake characteristics themselves, and uncertainty is associated with other lack of knowledge. In general, it is not considered possible to significantly reduce randomness by additional analysis or test based on current state-of-the-art techniques. Uncertainty, on the other hand, is considered to result primarily from analytical modeling assumptions and other lack

of knowledge concerning variables such as material strength, damping, etc., which could in many cases be reduced by additional study or test.

When developing the median ground acceleration, it is computationally convenient to work with a median factor of safety, $\hat{F}$, such that:

$$\hat{A} = \hat{F} A_{SSE} \quad (1)$$

where A_{SSE} is the peak ground acceleration associated with the Safe Shutdown Earthquake (SSE) or Design Basis Earthquake (DBE). The overall median factor of safety, $\hat{F}$, may in turn be broken down (separation of variables) into individual factors of safety representing the important variables contributing to the seismic capacity and response variables associated with each structure or component.

For equipment, the factor of safety can be modeled as the product of the three random variables.

$$F = F_C \cdot F_{RS} \cdot F_{RE} \quad (2)$$

The capacity factor, F_C, for the equipment is a product of a strength factor, F_S, and an inelastic energy absorption factor, F_μ. The strength factor, F_S, represents the ratio of ultimate strength to the stress calculated for A_{SSE}. In calculating the value of F_S, the non-seismic portion of the total load acting on the support is subtracted from the strength. The inelastic energy absorption factor, F_μ, is a measure of the strength of an element failing in a ductile mode beyond the yield strength or plastic hinge stress.

The structural response factor, F_{RS}, recognizes that in the design analyses, the structural response was computed using specific (often conservative) deterministic response parameters for the structure. The structural response factor, F_{RS}, is expressed as a product of the factors influencing the variability on building response.

$$F_{RS} = F_{SA} \cdot F_\delta \cdot F_M \cdot F_{SD} \cdot F_{SS} \quad (3)$$

including a spectral shape factor representing the ratio of the median site-specific ground response spectra to the ground spectra used for design, a damping factor representing the variability in response due to difference in actual damping and design damping, a modeling factor accounting for the uncertainty in response due to modeling assumptions, a factor to reflect the reduction of seismic input with depth of embedment of the structure, and a factor to account for the effect of soil-structure interaction.

Similarly, the equipment response factor, F_{RE}, includes a spectral shape factor (including the effects of peak floor response spectra broadening and smoothing, and artificial time history generation), an equipment damping factor, a modeling factor, a factor to account for conservatism in combining modal responses, and a factor to account for conservatism in combining earthquake components.

The approach to developing the civil structure fragility is essentially the same as for equipment fragilities except that no equipment response factor, F_{RE}, is included.

COMPONENT FRAGILITIES

Structure Response

The principal variables contributing to the structure response factor of safety, F_{RS}, include the considerations of the shape of the response spectra, structure and soil damping, modeling considerations, embedment effects, soil-structure interaction (SSI) effects, and earthquake directional component combinations. The basis for establishing the structural response factor of safety and variabilities as well as the structure seismic loads is the Quadrex soil-structure interaction model and analysis results described in Ref. [5].

Ground Response Spectra

The soil-structure interaction analysis was based on recommended ground response spectra developed by J. A. Blume (Ref. [6]) for the SRP site. Although not specifically stated, these spectra appear to be approximately median plus one standard deviation spectra (i.e., 84% nonexceedance). As a result of the radiation of energy from the base slab into the soil (radiation or geometric damping), very high equivalent modal damping ratios (20 to 40 percent of critical) are computed from the Quadrex soil-structure interaction analysis (Ref. [5]). An average factor of safety of about 1.08 results for the equivalent 20% to 40% damping over the 2 to 10 Hz frequency range of interest. In addition, the average ratio of the spectral acceleration developed by the artificial earthquake time history to the specified ground response spectral acceleration is about 1.08 over the frequency range of interest (1 to 5 Hz). The overall factor of

safety, F_{SA}, for the ground response spectra used in the analysis compared to the expected median value is about 1.08 x 1.08 or about 1.17.

Damping

A comparison of the damping values used in the Quadrex analysis and those expected in the range of severe building distress is:

	Damping (% Critical)	
	QUADREX	FRAGILITY
Structure	4	5
Soil Hysteretic	9	13
Geometric	7 to 27	7 to 27

The average damping factor of safety, F_s developed from the ratio of the spectral acceleration from the Quadrex analysis compared to spectral accelerations at the damping expected at structure or equipment failure of 1.02 was used.

Modeling

The factor of safety due to modeling is expected to be essentially unity with no randomness. A lognormal standard deviation for uncertainty, β_U, of 0.1 was estimated in order to account for mode shape effects.

Embedment

When a structure is embedded such as the L- and P-Reactors, the earthquake input at the base slab can be expected to be significantly reduced from the surface motion. Since the hazard curves are developed in terms of the free-field surface acceleration levels, a factor of safety, F_{SD}, was developed in order to reflect any conservatism expected in the response computed by Quadrex due to embedment as well as the variabilities associated with this factor.

In Ref. [5], a deconvolution analysis was performed to determine the expected seismic input at the base slab of the structure compared to the free-field surface input. These results are considered to be median-centered. However, because of licensing restrictions, the reduction in spectral acceleration was not allowed to decrease below 60 percent of the free-field acceleration in the Quadrex analysis. To prevent greater reduction, the response of the structure was multiplied by 1.3 in the Quadrex analysis. Consequently, a factor of safety of 1.3 is used in the fragility analysis based on the assumption that the Quadrex deconvolution analysis is essentially median-centered.

Soil-Structure Interaction

The soil-structure interaction analysis performed by Quadrex was conducted using current state-of-the-art techniques and is considered to be essentially median-centered. Variations due to possible changes in the soil shear modulus at shear strains above the SSE were accounted for in the factor of safety for modeling, F_M, and the effect of embedment was accounted for separately in F_{SD} as previously discussed.

Combined Structure Response Effects

The combined factor of safety, F_{RS}, and associated variabilities may then be developed for the above parameters. The combined factor of safety for the horizontal direction is 1.55. β_R is 0.18 and β_U is 0.31.

Structure Fragility

The primary lateral load-carrying system of the structure is of reinforced concrete construction. For reinforced concrete structures, the strength factor is a function of material strengths associated with the concrete and the reinforcing steel and relationships expressing strength of concrete walls in flexure and shear.

Strength of Concrete and Reinforcing Steel

Concrete for the L- and P-Reactor structures was specified to have a minimum compressive strength of 2500 psi at 28 days. The average 28-day strength for 2500 psi concrete was conservatively estimated to be approximately 3000 psi with a logarithmic standard deviation of 0.12. A factor of 1.2 was applied to the 28-day strength to develop the strength of the aged concrete, resulting in a median value of 3600 psi. A logarithmic standard deviation associated with aging was estimated to be 0.10. Combining the effects of average 28 day strength with subsequent aging gives an overall β_U of 0.16. Based on a survey of test results from other nuclear plants, the median yield strength, f_y, and logarithmic standard deviation, β_U, for the Grade 40 reinforcing steel are 47 ksi and 0.09, respectively.

Strength of Shear Walls in Flexure

Equations to predict the overturning (in-plane) moment capacity of rectangular shear walls containing uniformly distributed vertical reinforcement were derived from the basic ultimate strength design provisions for reinforced concrete members subjected to flexure and axial loads contained in the ACI code. These provisions are based upon the satisfaction of force

equilibrium and strain compatibility and have been verified by testing. Hence, they are judged to be median centered. Uncertainty in the median flexural strength is estimated to be β_U of 0.10 based on test data.

Shear Strength of Concrete Walls

Recent studies have shown that the shear strength of low-rise concrete shear walls with boundary elements are conservatively predicted by the ACI code provisions. Median shear strength which is based on test data of low rise walls is given by an equation from Ref. [3]. Based on an evaluation of the same experimental data, the logarithmic standard deviation of the median shear strength equations was estimated to be 0.15.

Structure Strength

A strength factor for this building is evaluated as the structure capacity as given in median flexure or shear provisions with median material properties divided by the corresponding shear and moment from the Quadrex soil-structure interaction analysis (Ref. [5]) for east-west earthquake ground shaking. The structure is much weaker against east-west ground motion.

Above El. 48, the building is a relatively strong box-type structure. Below El. 48 feet, the east-west running walls in the tower region are discontinued. There is a 5 foot thick roof slab at El. 48 feet, which extends to the north of the tower region about 110 feet to an expansion joint which structurally separates this portion of the building from additional structures to the north. In addition, this 5 foot thick slab extends to the south of the tower region to a 5 foot thick shear wall. Shear loads from the tower structure above and from the massive slab at El. 48 feet must be resisted by the shear walls to the south of the tower region and by out-of-plane bending of the underlying north-south running walls. The capacity of the building walls between Elevations 34 to 48 feet is a factor of 2.83 times the shear load at this elevation of the building.

Below El. 34 feet, there are additional shear walls at the southern portion of this building and to the northwest of the tower region to resist lateral forces. Consequently, the capacity/demand ratios for lateral load resisting elements from El. 0 to El. 34 feet are larger than for the resisting elements between El. 34 and 48 feet. In addition, capacity/demand ratios for elements above El. 48 feet are larger than 2.83.

The median capacity/demand ratio or strength factor for the L-Reactor building is 2.83 as described above. Uncertainty in this median factor results from the following sources: 1) material strength; 2) the strength relationship for shear; and 3) uncertainty introduced because a simple stick model was used to represent the complex load distribution. Combining all sources of uncertainty results in a total β_U of 0.22.

Structure Inelastic Energy Absorption

The Riddell-Newmark ductility modified response spectra approach (Ref. [1]) has been used to predict the inelastic energy absorption factor, F_μ, corresponding to the system ductility, μ. An effective ductility corresponding to shear wall structures and earthquake magnitudes on the order of 6 (i.e. $5.3 < M < 6.3$) has been used. The majority of seismic risk for the SRP plant is estimated to result from earthquakes in this magnitude range.

In order to estimate the system ductility, a story drift approach has been utilized, where system ductility is given by:

$$\mu = \frac{\sum_i W_i \Delta_{\mu,i}}{\sum_i W_i \Delta_{e,i}} \qquad (4)$$

where W_i is the story weight, $\Delta_{\mu,i}$ is the total story drift at failure, and $\Delta_{e,i}$ is the elastic story drift at yield level. The story drifts at failure are estimated by developing a structure deflected shape in which the story with the greatest amount of inelastic behavior (i.e. the smallest capacity/demand ratio) is set to a drift judged to correspond to failure with stories below deforming at yield level and stories above deforming in a manner which is compatible with the inelasticity lower in the structure. It is estimated that the median story drift corresponding to structural failure due to shear is 0.7 percent of the story height. Uncertainty is evaluated by taking 0.4 and 1 percent to be 10 and 90 percent probability levels. The deflected shape at yield is taken to be the deflected shape from the Quadrex analysis scaled by the minimum strength factor of 2.83. By this approach, the median inelastic energy absorption factor is evaluated to be 1.62.

Structure Capacity

The median capacity for the L-Reactor building can be approximated by the median response factor times the median strength factor times the median inelastic energy absorption factor times the design free-field ground acceleration (0.2g). In this manner, the fragility of the structure as represented by the median capacity, the logarithmic standard deviation associated with randomness, β_R, the logarithmic standard deviation associated with uncertainty, β_U, and the 95 percent confidence of 5 percent probability of failure (HCLPF) level are given by:

$\hat{A}$ = 1.42g

β_R = 0.18

β_U = 0.40

HCLPF = 0.55g

Equipment Fragilities

Heat Exchangers

The heat exchangers are horizontal, saddle-mounted cylindrical tanks; mounted on four wheel rail trucks; and located at elevation -20 feet. Seismic bracing has been added to the heat exchangers to provide resistance to overturning (transverse response) or rolling (longitudinal response). Bracing is bolted to the floor and to steel members connecting it to the heat exchanger. Provisions are made for either thin laminated steel shims or solid block shims at base plates and the top of the bents where the bracing is bolted to the floor and to the heat exchanger, respectively. The shims are significant because bending of the bolts at the base of the bracing which is permitted by thin laminated shims governs the seismic capacity of the heat exchanger.

The design basis loads were not available so seismic loads were recalculated using the Quadrex floor response spectra at Elev. -20. With the exception of potential failure of the anchor bolts protruding from the concrete floor, the factor of safety for all other failure modes was 4 or more. The controlling capacity for the heat exchangers was found to be the base plate anchor bolts. The capacity of these bolts is dependent on whether laminated shims or solid block shims are used since the joint behavior under lateral loads is different. For the case of a solid shim, the joint will slip a small amount until the clearances in the shim and plate bolt holes are reached at which time the bolt bears against the shim. For this case, the bolt is loaded in tension and shear but with very limited bending as shown in Figure 2a. For the case of thin shims, the bolt is free to displace laterally a relatively large amount to the point at which plastic hinges are formed at the top and bottom of the bolt. Plastic hinges are formed at a very low load level (about a factor of 0.63 times the loads developed from Quadrex floor spectra). However, the formation of plastic hinges does not constitute failure under transient earthquake loading. The joint will continue to slip until the bolt is stretched sufficiently to provide a clamping force between the shims which then carries the shear loads while the bolt is loaded in axial tension with bending at the base and sole plates. A sketch illustrating this behavior is shown in Figure 2b.

For the case of anchor bolts with solid shims, median capacity was evaluated in accordance with an interaction formula for combined shear and tension (bending is assumed to be negligible). The factor of safety for anchor bolts with solid shims is calculated to be 3.02. Combining the heat exchanger factor of safety and uncertainty with the response factor of safety, randomness, and uncertainty results in the following heat exchanger fragility (solid shim case):

$\hat{A}$ = 0.94g

β_R = 0.18

β_U = 0.33

HCLPF = 0.41g

For the case of the anchor bolts with thin shims, the ultimate shear capacity is given by the horizontal component of the bolt tension as the bolt has been displaced laterally, $P_{bolt} \sin\theta$ plus the clamping force on the shims times a coefficient of friction, $\mu(P_{bolt}\cos\theta - P_{seismic})$ The factor of safety on strength was therefore determined from the relationship:

$$F.S. = \frac{P_{bolt}(\sin\theta + \mu\cos\theta)}{V_{seismic} + \mu P_{seismic}} \qquad (5)$$

where θ is the angle formed by the offset and μ is the coefficient of friction between the shims and plates

The angle θ is related to the average bolt strain, ϵ_{bolt} by the following relation:

$$\cos\theta = \frac{1}{1 + \epsilon_{bolt}} \qquad (6)$$

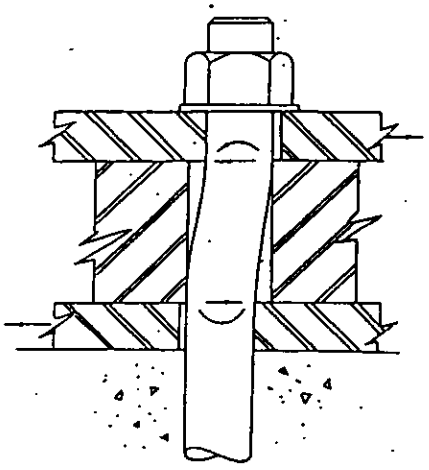

a. Solid Shims

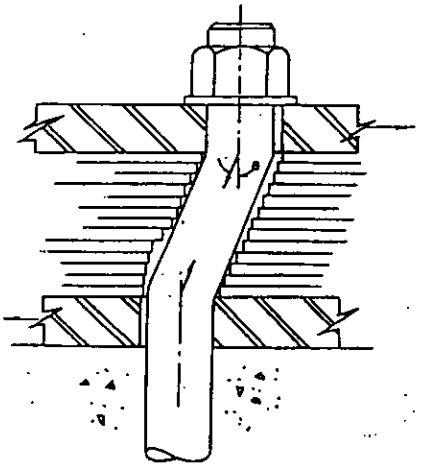

b. Thin, Laminated Shims

Figure 2 - Behavior of Shims

Based on a median coefficient of friction between the laminated shims of about 0.5 (steel on steel sliding friction) and an average strain over the bolt length of 1% at failure, a median factor of safety of the bolts of about 2.27 was calculated for the thin shim condition. Including the building response factor of safety and variabilities, the fragility for the thin shim condition is:

$\hat{A}$ = 0.70g

β_R = 0.18

β_U = 0.33

HCLPF = 0.30g

Main Tank

The main tank consists of top tube sheet, a bottom tube sheet, and a cylindrical tank. The top tube sheet is connected to the cylindrical tank wall by a flexible expansion joint and is supported from the concrete by bearing supports. The bottom tube sheet and cylindrical tank are supported on a separate set of bearing pads. Thus, the bottom tube sheet and tank can respond essentially independently from the top tube sheet during a seismic event. Seismic loads and stresses in the top tube sheet and nozzle system are much lower than in the main tank and bottom tube sheet assembly.

Six outlet nozzles are located just above the top plate of the bottom tube sheet. These nozzles are embedded in concrete. This provides a very stiff connection between the tank wall and the concrete which results in correspondingly high nozzle stresses occurring due to increased tank seismic displacements after failure of the bottom anchorage has occurred. The bottom tube sheet and tank assembly were modeled as part of the overall structure seismic model by Quadrex (Ref. [5]). Loads from this model were then applied to a detailed finite element model of a sector of the tank and nozzle. Seismic loads and stresses developed from these two analyses formed the basis of the fragility evaluation. Buckling of the tank wall was checked by Quadrex and found to have a very high factor of safety so that this mode of failure is not expected to control. Fragility of the main tank was based on failure of the nozzles in shear (i.e., trunnion loading). A factor of safety on strength of 3.3 with β_U of 0.14 were calculated for the main tank based on the above assumptions. Combining the factors of safety and variabilities for strength with those for structure and equipment response, the fragility for the main tank was evaluated as:

$\hat{A}$ = 1.04g

β_R = 0.20

β_U = 0.44

HCLPF = 0.36g

Pumps, Control Rods, & Forest

It was determined that these items are not contributors to the seismic risk of seismic indirect RCL pipe break when their capacities are compared to that of the main tank, heat exchangers, and building.

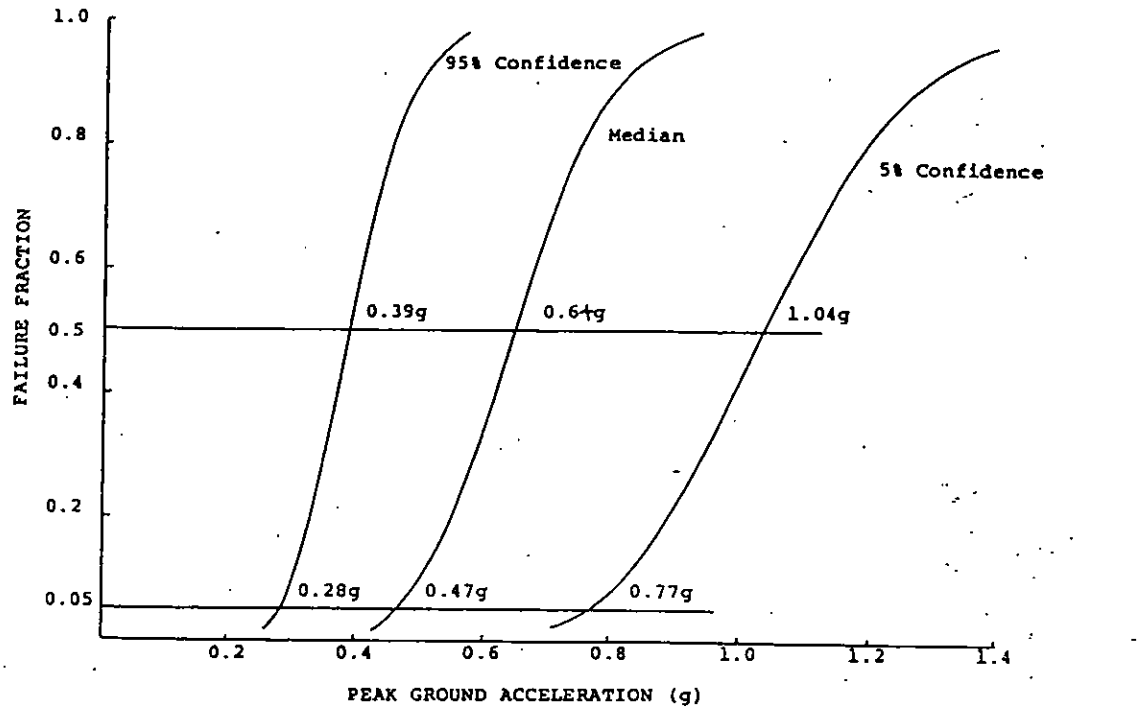

Figure 3 - Plant Fragility (Laminated Shims)

PLANT DAMAGE STATE FRAGILITIES

Plant damage state fragilities for seismic-induced indirect RCL pipe are developed from the individual component fragilities described in the previous section. Following the rules of Boolean algebra, the individual component fragilities were combined, two at a time, using the Discrete Probability Distribution (DPD) approach (Ref. [6]) to form plant damage state fragility curves. For plant damage states corresponding to seismic-induced indirect RCL pipe break, the Boolean expression is:

Pipe Break = Tank ∪ Heat Exch ∪ Bldg

indicating that the plant damage state consists of the union of the tank with the heat exchangers with the building.

With the DPD approach, the individual component fragility curves are first discretized into a family of fragility curves, each with a probabilistic weighting, representing the uncertainty (characterized by the β_U value) in the fragility evaluation. Each one of the, say n, curves of one component is then combined, according to the rules of Boolean algebra, with each one of the n curves of the second component. The resulting nxn curves are then condensed back to n curves, which are then combined with the n curves of the third component. This process is continued for all components in the Boolean expression, resulting in n plant damage state fragility curves.

Plant level fragility including heat exchangers with thin laminated shims, the tank, and the building with independent randomness and uncertainty for all components is a median acceleration capacity of about 0.64 g with a high confidence, low probability of seismic failure of about 0.28 g. A plant damage state fragility curve for the case of laminated shims is shown is Figure 3. If solid block shims are assumed, the median capacity increases to about 0.76 g with a HCLPF of about 0.33 g. If the heat exchangers are strengthened to the extent they do not influence the plant fragility, the median capacity increases to about 0.93 g with a HCLPF of 0.36 g.

SEISMIC RISK

The seismic risk of RCL pipe failure indirectly-induced by earthquakes is developed by a convolution of seismic hazard curves with fragility curves representing the plant damage states. For this study, the set of seismic hazard curves given in Figure 4 (from Ref. [4]) was used. The uncertainty in the earthquake hazard is accounted for by developing a family of curves and assigning a subjective weighting factor (in this case, 0.1) to each curve. Due to the high capacity of the plant fragilities, the hazard curves had to be extrapolated to lower annual frequency of exceedances than shown in Figure 4 in order to compute the low seismic risks. These curves were linearly extrapolated on semi-log paper down to 10^{-9} for this risk study. In addition, these extrapolated curves were truncated at 1.5 g peak ground acceleration, since hazard curves in excess of 1.5 g are not considered credible for the SRP site.

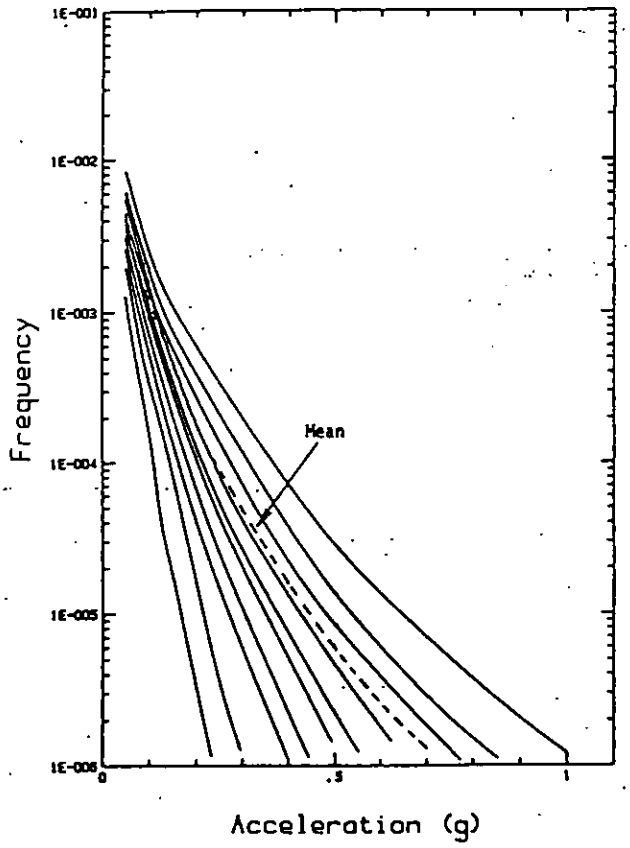

Figure 4 - Seismic Hazard Curves

In order to obtain the annual occurrence frequencies of the plant damage states, the family of plant damage state fragility curves discussed above are convolved with the family of seismic hazard curves. The convolution between the seismic hazard and the plant damage state fragility is carried out by selecting a hazard curve j and a fragility curve i; the probability assigned to the plant damage frequency resulting from the convolution is the product of the probabilities p_i and q_j assigned to these two curves. The convolution operation consists of multiplying the frequency of occurrence of an earthquake peak ground acceleration between a and a+da with the conditional frequency of the plant damage state, and integrating such products over the entire range of peak ground accelerations 0 to 1.5 g. Comparisons of the seismic risk of RCL Pipe Failure for several cases are shown in Table 1.

Table 1
L-Reactor Seismic Risk of RCL Pipe Failure

	Mean	Median	95% to 5% Confidence
Laminated Shims	6×10^{-6}	7.8×10^{-7}	3.3×10^{-5}-$<10^{-8}$
Solid Shims	2.9×10^{-6}	2.9×10^{-7}	1.6×10^{-5}-$<10^{-8}$
Upgraded HE	2.0×10^{-6}	7.4×10^{-8}	9.6×10^{-6}-$<10^{-8}$
HE & Tank Upgrade	2.9×10^{-7}	$<10^{-8}$	1.4×10^{-6}-$<10^{-8}$

Contribution to Seismic Risk from Different Acceleration Ranges

Ranges of acceleration which contribute most significantly to the overall frequency of occurrence of the damage state can be evaluated by integrating over small acceleration ranges and comparing the occurrence frequency obtained with that obtained by integrating over the entire range of accelerations. Figure 5 gives the percent contributions for mean risk from various acceleration ranges assuming a maximum credible peak ground acceleration of 1.5 g.

The contribution from the acceleration ranges below 0.25 g is very small for both the mean and median seismic risk. The majority of the mean risk results primarily from earthquakes with peak ground accelerations in the 0.25 g to 0.85 g range, centered about 0.4 g. Similarly, the median risk occurs primarily from earthquakes in the 0.35 to 1.5 g range and is centered at about 0.6 g. Seismic ground motions well in excess of the 0.2 g design level are required to produce substantial risk due to indirect pipe failure.

CONCLUSIONS

Building fragility, plant fragility (building, main tank, heat exchanger with laminated shims), and seismic risk for both L- and P-Reactors are compared in the Table 2. The seismic risk values shown are all quite low and are not substantially out-of-line with estimates for commercial nuclear power plants. Therefore, for seismic indirectly-induced pipe failure, no plant modifications appear warranted.

Table 2
L- and P-Reactor Seismic Fragilities & Risk

	L	P
Building Fragility		
Median Capacity (g)	1.42	0.89
HCLPF (g)	0.55	0.34
Plant Fragility		
Median Capacity (g)	0.64	0.59
HCLPF (g)	0.28	0.27
Seismic Risk		
Mean Frequency of Failure	6.0×10^{-6}	7.6×10^{-6}
Median Frequency of Failure	7.8×10^{-7}	1.3×10^{-6}
95% Upper Confidence Bound	3.3×10^{-5}	4.1×10^{-5}

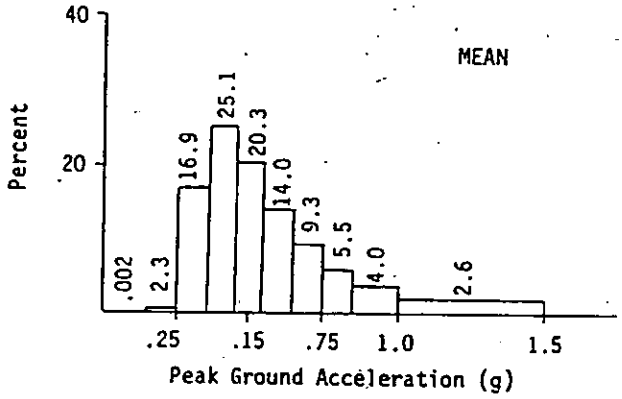

Figure 5 - Contribution to Risk of Different Acceleration Ranges

REFERENCES

[1] Riddell, R., and N. M. Newmark, "Statistical Analysis of the Response of Nonlinear Systems Subjected to Earthquakes", Department of Civil Engineering, **Report UILU 79-2016**, Urbana, Illinois, August 1979.

[2] Kaplan, S., **On the Method of Discrete Probability Distributions in Risk and Reliability Calculations, Risk Analysis**, 1981.

[3] Barda, F., J. M. Hanson and W. G. Corley, "Shear Strength of Low-Rise Walls with Boundary Elements", ACI Symposium, "Reinforced Concrete Structures in Seismic Zones", ACI, Detroit, Michigan, 1976.

[4] McCann, M. W. Jr., **Historic Seismicity Analysis for the Savannah River Site,** JBA 153-010-02 prepared for E. I. du Pont de Nemours & Company, Inc., April 1986.

[5] Tang, C. C., **Seismic Analysis of 'L' Reactor Buildings at the Savannah River Site,** QUAD-1-85-016, Vol. I, for E. I. du Pont de Nemours and Company, November 1985.

[6] URS/John A. Blume & Associates, Engineers, "Update of Seismic Criteria for the Savannah River Plant," for E. I. du Pont de Nemours & Company, September 1982.

ACKNOWLEDGMENT

The information contained in this article was developed during the course of work done under Contract No. DE-AC09-76SR00001 (now Contract No. DE-AC09-88SR18035) with the U. S. Department of Energy.